Boson-fermion mixtures inside an elongated cigar-shaped trap

Z. Akdeniz^{1,2}, P. Vignolo¹‡ and M. P. Tosi¹

¹NEST-INFM and Classe di Scienze, Scuola Normale Superiore, I-56126, Pisa, Italy ²Department of Physics, Istanbul University, Istanbul, Turkey

Abstract. We present mean-field calculations of the equilibrium state in a gaseous mixture of bosonic and spin-polarized fermionic atoms with repulsive or attractive interspecies interactions, confined inside a cigar-shaped trap under conditions such that the radial thickness of the two atomic clouds is approaching the magnitude of the s-wave scattering lengths. In this regime the kinetic pressure of the fermionic component is dominant. Full demixing under repulsive boson-fermion interactions can occur only when the number of fermions in the trap is below a threshold, and collapse under attractive interactions is suppressed within the range of validity of the mean-field model. Specific numerical illustrations are given for values of system parameters obtaining in ⁷Li-⁶Li clouds.

PACS numbers: 03.75.-b, 05.30.-d, 73.43.Nq

1. Introduction

Dilute boson-fermion mixtures have been studied in several experiments by trapping and cooling gases of mixed alkali-atom isotopes [1, 2, 3, 4, 5, 6]. The boson-fermion coupling strongly affects the equilibrium properties of the mixture and can lead to quantum phase transitions (for a review see [7]). In particular, boson-fermion repulsions in three-dimensional (3D) clouds can induce spatial demixing of the two components when the interaction energy overcomes the kinetic and confinement energies [8]. This occurs in 3D if the fermion density is high or if the boson-fermion repulsion is strong, as shown in a phase diagram obtained by imposing pressure balance and equality of chemical potentials in coexisting phases [9, 10]. Although spatial demixing has not yet been experimentally observed, the experiments of Schreck et al. [1] on ⁷Li-⁶Li mixtures inside an elongated 3D trap appear to be close to the onset of a demixed state [11]. Collapse driven by increasing the number of bosons in a 3D trap has instead been observed in ⁸⁷Rb-⁴⁰K mixtures [5], where the interspecies interactions are attractive.

On approaching a quasi-two-dimensional (Q2D) situation, the Fermi energy starts to increase linearly with the number of fermions per unit area, so that the linear stability condition of the mixture becomes independent of the fermion density and involves only the scattering lengths and the transverse width of the cloud. In this regime spatial demixing of a ⁷Li-⁶Li gas is predicted to occur by simply squeezing down the axial thickness of the atomic clouds [12].

The analysis of Viverit et al. [9] for homogeneos boson-fermion matter has been extended by Das [13] to a one-dimensional (1D) homogeneous mixture. In the 1D case the Fermi energy is proportional to the square of the number of fermions per unit length, so that the mixed state becomes unstable at low linear fermion densities. The dependence of the kinetic pressure of the Fermi gas on the fermion density becomes stronger with decreasing dimensionality, and in 1D a number of fermions above a threshold will want to occupy the whole available space irrespectively of the repulsions exerted by the bosons. Similarly, it is easily shown that a 1D homogeneous mixture with attractive boson-fermion interactions is stabilized against collapse by the Fermi pressure if the linear density of fermions is above the same threshold.

In this paper we examine the instabilities of a dilute boson-fermion mixture trapped inside a strongly elongated harmonic confinement. We give the general conditions under which various forms of demixing can occur in a Q1D confined geometry in terms of the physical parameters of the system and draw a phase diagram at zero temperature in a plane defined by two scaling parameters. We support our analysis by extensive mean-field calculations of the equilibrium density profiles in a ⁷Li-⁶Li mixture. We find that in the case of interspecies repulsions the stability condition which applies in the macroscopic limit is still approximately valid for full demixing in harmonic confinement. We next turn to the case of attractive interspecies interactions, where we search for a collapse instability by a variational approach patterned after the work carried out by Miyakawa et al. [14] on a 3D mixture. We find that our mean-field model does not allow

collapse in a confined Q1D geometry, but only predicts that the density profiles keep narrowing with increasing attractive coupling strength until the validity of the model is lost. These predictions of the variational analysis are again supported by numerical illustrations of density profiles.

The paper is organized as follows. In Sec. 2 we describe the mean-field model and report the stability condition for a macroscopic mixture in 1D and Q1D geometry. Section 3 discusses the conditions under which various forms of demixing occur in a Q1D harmonic confinement and shows some illustrative configurations of the density profiles in the gaseous cloud in the phase-separated regime. The variational analysis and some illustrative density profiles for the case of interspecies attractions are given in Sec. 4. Finally, Sec. 5 gives a summary and some concluding remarks.

2. The model and the phase diagram

The atomic clouds are trapped in cigar-shaped potentials given by

$$V_{b,f}^{ext}(x,y,z) = m_{b,f}\omega_{\perp(b,f)}^2(x^2 + y^2)/2 + m_{b,f}\omega_{z(b,f)}^2 z^2/2 \equiv U_{b,f}(x,y) + V_{b,f}(z)$$
(1)

where $m_{b,f}$ are the atomic masses and $\omega_{z(b,f)} \ll \omega_{\perp(b,f)}$ the trap frequencies. We assume repulsive interactions between the bosons and focus on the case where the trap is elongated enough that the dimensions of the atomic clouds in the radial plane, which are of the order of the radial harmonic-oscillator lengths $a_{\perp(b,f)} = (\hbar/m_{b,f}\omega_{\perp(b,f)})^{1/2}$, are comparable to the magnitude of the 3D boson-boson and boson-fermion scattering lengths, a_{bb} and $|a_{bf}|$. In this regime we can study the equilibrium properties of the mixture at essentially zero temperature $(T \simeq 0.02 \, T_F)$ in terms of the particle density profiles along the z axis, which are $n_c(z)$ for the Bose-Einstein condensate and $n_f(z)$ for the fermions. The profiles are evaluated using the Thomas-Fermi approximation for the condensate and the Hartree-Fock approximation for the spin-polarized fermions. Here and in the following we shall take $a_{\perp b} = a_{\perp f}$ (= a_{\perp} , say).

The Thomas-Fermi approximation assumes that the number of condensed bosons is large enough that the kinetic energy term in the Gross-Pitaevskii equation may be neglected [15]. It yields

$$n_c(z) = [\mu_b - V_b(z) - g_{bf} n_f(z)]/g_{bb}$$
(2)

for positive values of the function in the square brackets, and zero otherwise. Here, μ_b is the chemical potential of the bosons. This mean-field model is valid when the high-diluteness condition $n_c a_{bb} \ll 1$ holds and the temperature is outside the critical region. If the conditions $a_{\perp} > (a_{bb}, |a_{bf}|)$ are fulfilled, the atoms experience collisions in three dimensions and the coupling constants in Eq. (2) can be written in terms of those for a 3D cloud as [16, 17]

$$g_{bb} = \frac{g_{bb}^{3D}}{2\pi a_{\perp}^2} , \quad g_{bf} = \frac{g_{bf}^{3D}}{2\pi a_{\perp}^2}$$
 (3)

with $g_{bb}^{3D} = 4\pi\hbar^2 a_{bb}/m_b$, $g_{bf}^{3D} = 2\pi\hbar^2 a_{bf}/m_r$ and $m_r = m_b m_f/(m_b + m_f)$.

The Hartree-Fock approximation [18, 19, 20] treats the fermion cloud as an ideal gas subject to an effective external potential, that is

$$n_f(z) = \int \frac{dp}{2\pi\hbar} \left\{ \exp\left[\left(\frac{p^2}{2m_f} + V^{eff}(z) - \mu_f\right)/k_B T\right] + 1 \right\}^{-1}, \tag{4}$$

where μ_f is the chemical potential of the fermions and

$$V^{eff}(z) = V_f(z) + g_{bf}n_c(z). \tag{5}$$

The fermionic component has been taken as a dilute spin-polarized gas, for which the fermion-fermion s-wave scattering processes are inhibited by the Pauli principle and p-wave scattering is negligibly small [21]. In the mixed regime the Fermi wave number in the axial direction and the condensate density should be smaller than $1/|a_{bf}|$, but this is not a constraint in the regime of demixing where the boson-fermion overlap is rapidly dropping. On the contrary, for large attractive interactions this condition, together with the diluteness condition $n_c a_{bb} \ll 1$, may not be fulfilled and this sets the range of validity of our results.

The chemical potentials $\mu_{b,f}$ characterise the system in the grand-canonical ensemble and are determined by requiring that the integrals of the densities over the z axis should be equal to the average numbers N_b and N_f of particles. The presence of a bosonic thermal cloud can be treated by a similar Hartree-Fock approximation [11], but it has quite negligible effects at the temperatures of present interest.

As the boson-fermion coupling increases, the mixture can become unstable against demixing (in the case $g_{bf} > 0$) or collapse (in the case $g_{bf} < 0$). In the macroscopic 1D limit at given particle densities a linear stability analysis based on a mean-field energy functional predicts that the locations for demixing and collapse coincide and that the gaseous cloud is stable if the usual condition

$$g_{bb}g_{ff} - g_{bf}^2 \ge 0 \tag{6}$$

is fulfilled [9], with $g_{ff} = \hbar^2 \pi^2 n_f/m_f$ playing the role of an effective fermion-fermion repulsion due to the Pauli pressure in the Fermi gas. Since g_{ff} increases with n_f , the mixed state is stable at given boson-fermion attractive or repulsive coupling strength if the linear density of fermions is *above* a threshold [13].

The stability condition in Eq. (6) can be extended to the Q1D geometry for large numbers of particles and if the boson and fermion densities vary smoothly (for the sake of brevity in the following we will refer to this regime as the "Q1D macroscopic limit"). By using Eq.(3) for the boson-boson and boson-fermion couplings and by taking the value of n_f as the linear fermion density at the centre of the trap, Eq. (6) is rewritten as

$$\frac{|a_{bf}|}{a_{\perp}} \le \left(\frac{2\pi m_r^2}{m_b m_f} k_f a_{bb}\right)^{1/2} \tag{7}$$

where $k_f = (2N_f)^{1/2}/a_{zf}$ is the Fermi wave number under harmonic confinement at the centre of the trap, with a_{zf} the axial oscillator length for the fermions. In Fig. 1 we have plotted Eq. (7) in the plane $\{|a_{bf}|/a_{\perp}, k_f a_{bb}\}$ for the case of a ⁷Li-⁶Li mixture.

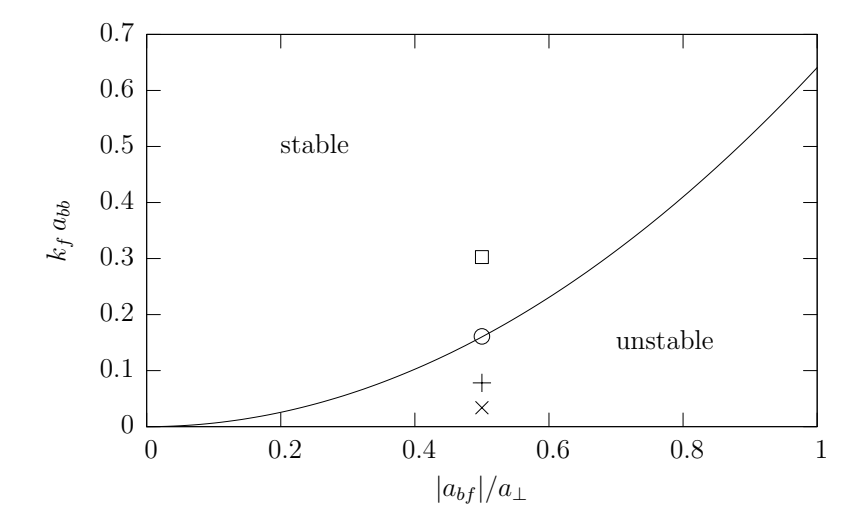


Figure 1. Phase diagram of a Q1D ⁷Li-⁶Li mixture at T=0, in the plane defined by the dimensionless parameters $a_{bb}k_f$ and $|a_{bf}|/a_{\perp}$. The symbols at $|a_{bf}|/a_{\perp}=0.5$ correspond to the parameters of the configurations shown in Figs. 3 and 6: (\square) $N_f=3\times10^5$, (O) $N_f=8,5\times10^4$, (+) $N_f=2\times10^4$, (×) $N_f=3740$.

The effects of finite size and dishomogeneity of the gaseous clouds are not taken into account in Eq. (7), with the consequence that the resulting phase diagram in Fig. 1 shows a sharp transition as in the macroscopic limit. Transitions in a mesoscopic cloud under confinement are instead spread out and several alternative definitions of their location can therefore be given. These are discussed in the next two sections. We shall for the sake of brevity continue to use expressions such as "phase transitions" and "phase diagram" when needed.

3. Spatial demixing

In the calculations that we report in the following we have used values of the trap frequencies appropriate to the experiments in Paris on the $^{7}\text{Li-}^{6}\text{Li}$ mixture [1], that is $\omega_{zb}/2\pi = 4000$ Hz and $\omega_{zf}/2\pi = 3520$ Hz. We also take $a_{bb} = 5.1\,a_{0}$, a_{0} being the Bohr radius, as appropriate to $^{7}\text{Li-}^{7}\text{Li}$ s-wave scattering. We first discuss in this Section three alternative locations of the demixing point in a mesoscopic trapped cloud, that we denote as partial, dynamical, and full demixing. Their definition and the derivation of simple analytical expressions in the Q1D model are given below.

3.1. Partial demixing

The interaction energy E_{int} between the boson and fermion clouds initially grows as the boson-fermion coupling is increased, but in the demixing regime reaches a maximum and then falls off as the overlap between the two separating clouds diminishes. We locate partial demixing at the maximum of E_{int} , that we calculate from the density profiles

according to the expression

$$E_{int} = g_{bf} \int dz \, n_c(z) n_f(z). \tag{8}$$

The behaviour of the interaction energy as a function of a_{bf} at $a_{\perp} = 38 a_0$, and for various numbers of bosons and fermions, is shown in Fig. 2.

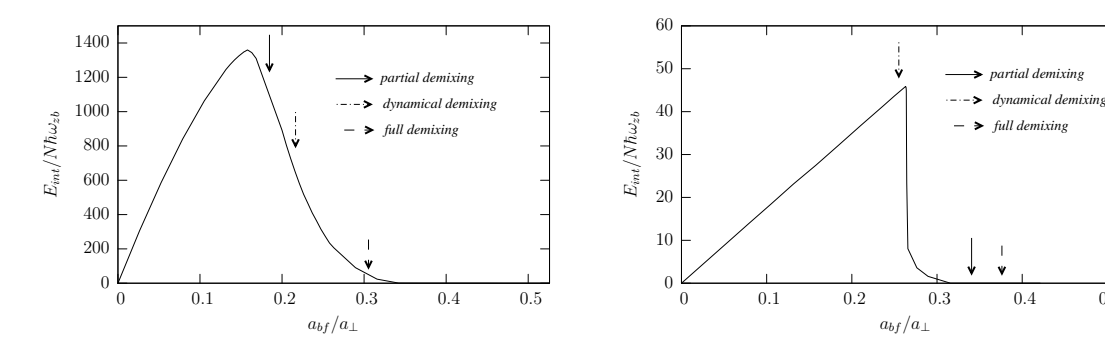


Figure 2. Boson-fermion interaction energy E_{int} (in units of $N\hbar\omega_{zb}$, with $N=N_b+N_f$), as a function of a_{bf} (in units of a_{\perp}) for $a_{bb}=5.1\,a_0$. Left panel: $N_b=N_f=10^4$. Right panel: $N_b=100$ and $N_f=19900$. The arrows indicate the locations of demixing estimated from Eqs. (9), (13), and (14).

An approximate analytic formula for the location of partial demixing as a function of the system parameters in the Q1D model can be obtained from the condition $\partial E_{int}/\partial g_{bf}=0$ which leads to the relation $n_c(z)n_f(z)-n_f^2(z)/g_{bb}-n_c^2(z)/g_{ff}=0$. By using the estimate $n_{c,f}\approx N_{b,f}/(2R_{b,f})$ with the values of the cloud radii in the absence of boson-fermion interactions, $R_f=(2N_f)^{1/2}a_{zf}$ and $R_b=[3N_bg_{bb}a_{zb}/(2\hbar\omega_{zb})]^{1/3}a_{zb}$, where $a_{z(b,f)}=(\hbar/m_{b,f}\omega_{z(b,f)})^{1/2}$, the location of the maximum in the boson-fermion interaction energy as a function of a_{bf}/a_{\perp} is found to lie at

$$\left. \frac{a_{bf}}{a_{\perp}} \right|_{part} \simeq \left(c_1 k_f a_{bb} + \frac{c_2}{k_f^2 a_{bb}^2} \right)^{-1} \tag{9}$$

where we have defined

$$c_1 = \frac{1}{4N_b^{2/3}} \frac{m_b a_{zb}}{m_r a_\perp} \left(\frac{3a_{bb} a_{zb}}{a_\perp^2}\right)^{1/3},\tag{10}$$

$$c_2 = \frac{8N_b^{2/3}}{\pi^2} \frac{m_f a_{bb}}{m_r a_{zb}} \left(\frac{a_{bb}^2}{3a_{\perp} a_{zb}}\right)^{1/3}.$$
 (11)

The prediction obtained from Eq. (9) is shown in Fig. 2 by solid arrows. For the case $N_b = N_f = 10^4$, there clearly is reasonable agreement between the analytical estimate and the numerical results. For a low number of bosons and a large number of fermions the condition given in Eq. (9) is dominated by the term involving c_1 . In this limit, the bosonic density is largely deformed by the pressure of the fermions and the prediction obtained from Eq. (9) overestimates the position of the maximum of the interaction energy (see right panel in Fig. 2).

3.2. Dynamical demixing

At some value of the boson-fermion coupling the fermion density vanishes at the centre of the trap. This occurs when

$$\frac{g_{bf}}{g_{bb}}\bigg|_{dun} = \frac{\mu_f}{\mu_b}.\tag{12}$$

We denote this point as the dynamical location of demixing in a mesoscopic cloud, since we expect a sharp upturn of the low-lying fermion-like collective mode frequencies to occur at this point, where the topology of the cloud changes. This has been shown to the case for both collisional and collisionless excitations in a mixture under 3D confinement [22, 23].

If we insert the chemical potentials for ideal-gas clouds in Eq. (12), we obtain an approximate expression for the location of dynamical demixing,

$$\left. \frac{a_{bf}}{a_{\perp}} \right|_{dun} \simeq \left(\frac{\pi m_r^2}{m_b m_f} k_f a_{bb} \right)^{1/2}. \tag{13}$$

The prediction obtained from Eq. (13) is indicated in Fig. 2 by dot-dashed arrows. For both small and large values of the number of bosons, the dynamical condition for demixing is in good agreement with the numerical results from the boson-fermion interaction energy.

3.3. Full demixing

The point of full demixing is reached when the boson-fermion overlap becomes negligible as in a phase transition occurring in a macroscopic cloud. If we use the stability criterion given in Eq. (7) for the macroscopic Q1D case, the condition for full phase separation at T=0 inside a strongly elongated trap is given by

$$\left. \frac{a_{bf}}{a_{\perp}} \right|_{full} \simeq \left(\frac{2\pi m_r^2}{m_b m_f} k_f a_{bb} \right)^{1/2} \tag{14}$$

or $a_{bf}|_{full} \simeq \sqrt{2}a_{bf}|_{dyn}$. The prediction obtained from Eq. (14) is indicated in Fig. 2 by short-dashed arrows. Analogously to the partial demixing condition there is better agreement with the numerical results on the boson-fermion interaction energy when the number of bosons is relative large.

In summary, in Q1D a small number of fermions allows demixing, which is in contrast to the case for full phase separation in 3D where the critical value of the boson-fermion scattering length decreases by increasing the number of fermions [9, 10], and to the Q2D case where the transition is controlled only by the geometrical parameters of the trap and not by the number of atoms [12].

The critical coupling strength for both dynamical and full demixing under harmonic confinement moves upwards with the law $g_{bf} \propto N_f^{1/4}$ as N_f increases, till the mixture becomes stabilized by the kinetic pressure of the fermions.

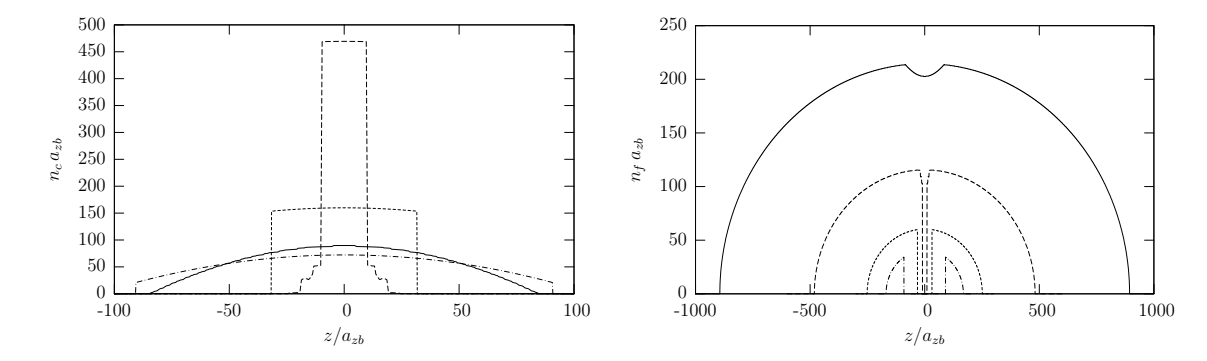


Figure 3. Density profiles of the condensate (left panel) and of the fermions (right panel) at $a_{bf}/a_{\perp} = 0.5$ for various numbers of fermion atoms: $N_f = 3 \times 10^5$ (solid line), $N_f = 8.5 \times 10^4$ (dashed line), $N_f = 2 \times 10^4$ (short-dashed line), and $N_f = 3740$ (dotted-dashed line). Notice the difference of the horizontal scales in the two panels.

3.4. Density profiles at full demixing

With the aim of verifying the validity of the condition of full component separation in Eq. (14), we have evaluated the boson and fermion density profiles by varying the boson-fermion scattering length as might be attained experimentally by exploiting optically or magnetically induced Feshbach resonances [24], or by varying N_f i.e. k_f at fixed radial size $a_{\perp} = 38 a_0$. As illustrative examples we show in Fig. 3 the density profiles of the lowest-energy configurations indicated by the symbols in Fig. 1. In agreement with the location of the configurations in the phase diagram, density profiles with a small number of fermions are spatially demixed, whereas stability is reached on increasing the number of fermions.

In the region of instability we have also found in addition to the thermodynamically stable configurations, shown in Fig. 3, various metastable "exotic" configurations for the demixed clouds. Some illustrative examples of such metastable density profiles, which break axial symmetry and/or consist of alternating slices of bosons and fermions, are shown in Fig. 4.

4. Collapse

In the case of attractive boson-fermion interactions we have studied the instabilities of the Q1D harmonically trapped mixture by a variational method. Following Miyakawa et al. [14], we write the total energy of the gas as a function of the boson order parameter $\Phi(z)$, with $|\Phi(z)|^2 = n_c(z)$, and of the fermion density distribution $n_f(z)$ as

$$E[\Phi(z), n_f(z)] = \int dz \left[\frac{\hbar^2}{2m_b} |\nabla \Phi(z)|^2 + V_b(z) |\Phi(z)|^2 + \frac{g_{bb}}{2} |\Phi(z)|^4 \right]$$

$$+ \int dz \left[\frac{\hbar^2 \pi^2}{6m_f} n_f^3(z) + V_f(z) n_f(z) + g_{bf} n_f(z) |\Phi(z)|^2 \right].$$
 (15)

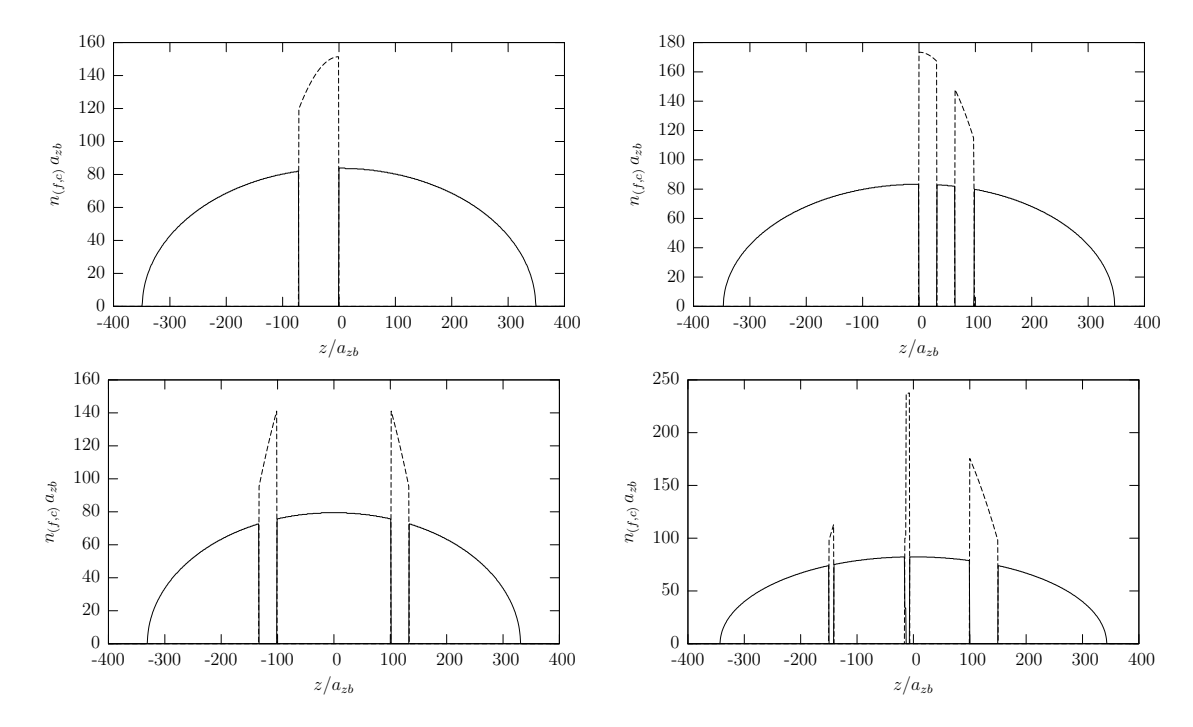


Figure 4. Metastable density profiles of fermions (solid line) and bosons (dashed line) at full demixing, for a Q1D mixture of $N_b = 10^4$ bosons and $N_f = 4 \times 10^4$ fermions with $a_{bb} = 5.1 \, a_0$, $a_{bf} = 19 a_0$, and $a_{bf}/a_{\perp} = 0.5$. The various configurations correspond to an excess energy $\Delta E/E$ over the thermodynamically stable demixed configuration given by $\Delta E/E \simeq 0.2\%$ (left-top panel), $\Delta E/E \simeq 1\%$ (right-top panel), $\Delta E/E \simeq 1.6\%$ (left-bottom panel), and $\Delta E/E \simeq 5\%$ (right-bottom panel).

We make a Thomas-Fermi Ansatz for the boson order parameter,

$$\Phi(\tilde{z};R) = a_{zb}^{-1/2} \left[\frac{3N_b}{4R} \left(1 - \frac{\tilde{z}^2}{R^2} \right) \right]^{1/2}$$
 (16)

where $\tilde{z} = z/a_{zb}$ and the variational parameter R is the dimensionless Thomas-Fermi radius of the condensate. Minimization of the free energy $E[\Phi(z), n_f(z)] - \mu_f(R)n_f(z)$ yields the fermion density distribution

$$n_f(\tilde{z};R) = \frac{2N_f}{\pi \lambda a_{zf}} \left(1 - \frac{\tilde{z}^2}{\lambda^2} \right)^{1/2},\tag{17}$$

where $\lambda \simeq N_f^{1/2} [8R^3/(3\tilde{g}_{bf}N_b)]^{1/4}$ is the turning point for the fermions at large interaction strength $\tilde{g}_{bf} = |g_{bf}|/(a_{zb}\hbar\omega_{zb})$. Finally, assuming that $\lambda > R$, *i.e.* as long as the fermion cloud is much broader than the bosonic one, the total energy E(R) becomes

$$\frac{E(R)}{\hbar\omega_{zb}} \simeq \frac{3\pi N_b}{16R^2} + \left(\frac{3m_f\omega_f^3}{2m_b\omega_b^3}\right)^{1/2} (\tilde{g}_{bf}N_b)^{1/2} \frac{N_f^2}{4R^{3/2}} + \frac{3g_{bb}N_b^2}{10R\,a_{zb}\,\hbar\omega_b} + \left(\frac{3\tilde{g}_{bf}}{8}\right)^{1/4} \frac{5N_b^{5/4}N_f^{1/2}g_{bf}}{4\pi R^{3/4}a_{zf}\hbar\omega_b} + \frac{\omega_f N_f^2}{\sqrt{24}\omega_b(\tilde{g}_{bf}N_b)^{1/2}} R^{3/2} + \frac{N_b}{10}R^2. \tag{18}$$

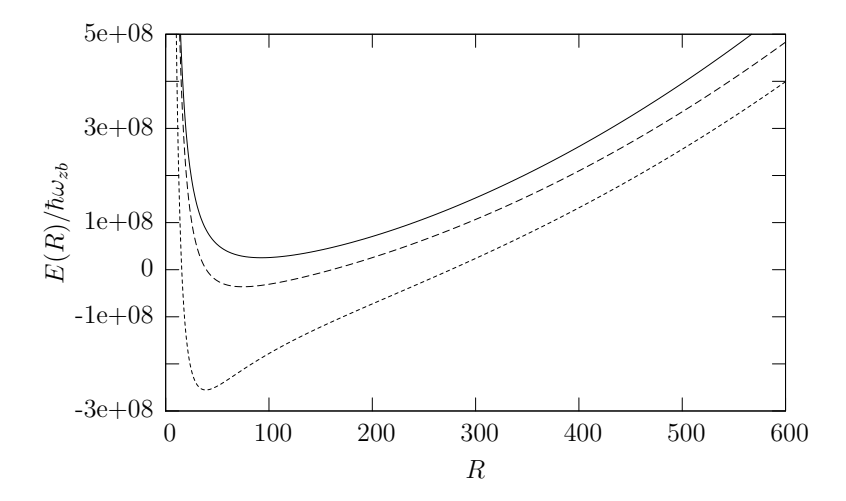


Figure 5. Energy E(R) (in units of $\hbar\omega_{zb}$) of a boson-fermion cloud in Q1D harmonic confinement, as a function of the variational parameter R for $N_b = N_f = 10^4$. The curves correspond to $a_{bf}/a_{\perp} = -0.26$ (solid line), -0.5 (dashed line), and -1 (short-dashed line).

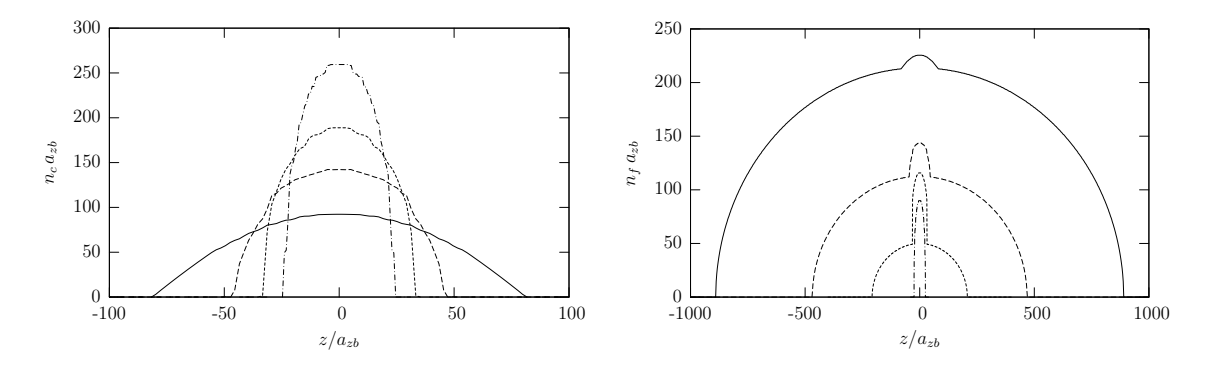


Figure 6. Density profiles of the condensate (left panel) and of the fermions (right panel) at $a_{bf}/a_{\perp} = -0.5$ for various numbers of fermion atoms: $N_f = 3 \times 10^5$ (solid line), $N_f = 8.5 \times 10^4$ (long-dashed line), $N_f = 2 \times 10^4$ (short-dashed line), and $N_f = 3740$ (dotted-dashed line).

The validity of this expression is limited by the diluteness condition $2Ra_{zb} \gg N_b \max(a_{bb}, |a_{bf}|)$.

Contrary to the 3D case, in Q1D the boson-fermion attraction energy does not modify the leading term of E(R) in the small-R region, so that E(R) remains positive and for $R \to 0$ (see Fig. 5). The mean-field model only leads to narrower and narrower density profiles, until pressure is relieved by the expulsion of atoms from the trap through three-body processes allowing collapse to proceed further. Some illustrations of mean-field density profiles in correspondence to the symbols shown in Fig. 1 is given in Fig. 6. The condensate density increases at the centre of the trap with a decrease in the number of fermions, which is thus seen to favour collapse.

5. Summary and concluding remarks

In summary, we have evaluated a mean-field description of a boson-fermion mixture confined inside a cigar-shaped trap, such that the scattering events can still be considered as three-dimensional but nevertheless affected by the radial confinement. We have focussed on the equilibrium properties of the mixture and in the macroscopic limit we have given a universal phase diagram for the transitions to demixing or collapse expressed in terms of scaling parameters of the system.

We have studied the boson-fermion interaction energy in a mesoscopic cloud as a function of a boson-fermion repulsive coupling and have given approximate analytical expressions identifying three critical regimes: (i) partial demixing where the boson-fermion interaction energy attains maximum value from a balance between increasing interactions and diminishing overlap; (ii) dynamical demixing where the fermionic density drops to zero at the centre of the trap and a sharp dynamical signature of demixing may be expected; and (iii) full demixing where the boson-fermion overlap is negligible as in the macroscopic limit. It is remarkable that in this model full demixing can be reached by simply *decreasing* the number of trapped fermions. In the region of phase separation we have found several metastable configurations for the demixed cloud, having various topologies but lying at higher energy above the stable configuration which is composed of a core of condensed bosons surrounded by fermions.

When the boson-fermion interaction is instead attractive, a Q1D mixture reaches collapse in the macroscopic limit under the same conditions as it attains full demixing for repulsive coupling, *i.e.* upon *lowering* the fermion density. While a mean-field treatment is clearly unable to describe the full path to collapse, we have seen that it supports the above view. It would be interesting to study the Q1D mixture with strong attractive interactions by using models beyond mean-field and with inclusion of three-body collisions.

This work was partially supported by an Advanced Reasearch Initiative of Scuola Normale Superiore (SNS). One of us (Z.A.) thanks SNS for a Visiting Grant and acknowledges support from TUBITAK and from the Research Fund of the University of Istanbul under Project Number BYP-118/12122002.

- Schreck F, Khaykovich L, Corwin K L, Ferrari G, Bourdel T, Cubizolles J and Salomon C 2001 Phys. Rev. Lett. 87 080403.
- [2] Goldwin J, Papp S B, DeMarco B and Jin D S 2002 Phys. Rev. A 65 021402.
- [3] Hadzibabic Z, Stan C A, Dieckmann K, Gupta S, Zwierlein M W, Görlitz A and Ketterle W 2002 Phys. Rev. Lett. 88 160401.
- [4] Roati G, Riboli F, Modugno G and Inguscio M 2002 Phys. Rev. Lett. 89 150403.
- [5] Modugno G, Roati G, Riboli F, Ferlaino F, Brecha R J and Inguscio M 2002 Science 297 2240.
- [6] Ferlaino F, Brecha R J, Hannaford P, Riboli F, Roati G, Modugno G and Inguscio M 2003 J. Opt. B 5 S3.
- [7] Vignolo P and Tosi M P, 2005 in press.
- [8] Mølmer K 1998 Phys. Rev. Lett. **80** 1804.
- [9] Viverit L, Pethick C J and Smith H 2000 Phys. Rev. A 61 053605.
- [10] Akdeniz Z, Minguzzi A, Vignolo P and Tosi M P 2002 Phys. Rev. A 66 013620.
- [11] Akdeniz Z, Vignolo P, Minguzzi A and Tosi M P 2002 J. Phys. B 35 L105.
- [12] Akdeniz Z, Vignolo P and Tosi M P, 2004 Phys. Lett. A 331 258.
- [13] Das K K 2003 Phys. Rev. Lett. **90** 170403.
- [14] Miyakawa T, Suzuki T and Yabu H 2001 Phys. Rev. A 64 033611.
- [15] Baym G and Pethick C J 1996 Phys. Rev. Lett. 76 6.
- [16] Salasnich L, Parola A and Reatto L 2002 Phys. Rev. A 65 043614.
- [17] Akdeniz Z, Minguzzi A and Vignolo P 2003 Laser Physics 13 577.
- [18] Minguzzi A, Conti S and Tosi M P 1997 J. Phys.: Condens. Matter 9 L33.
- [19] Amoruso M, Minguzzi A, Stringari S, Tosi M P and Vichi L 1998 Eur. Phys. J. D 4 261.
- [20] Vignolo P, Minguzzi A and Tosi M P 2000 Phys. Rev. A 62 023604.
- [21] DeMarco B, Bohn J L, Burke Jr. J P, Holland M and Jin D S 1999 Phys. Rev. Lett. 82 4208.
- [22] Capuzzi P, Minguzzi A and Tosi M P 2003 Phys. Rev. A 67 053605.
- [23] Capuzzi P, Minguzzi A and Tosi M P 2003 Phys. Rev. A 68 033605.
- [24] Inouye S, Goldwin J, Olsen M L, Ticknor C, Bohn J L and Jin D S 2004 Phys. Rev. Lett. 93, 183201.